On the Electronic Structure of NLi$_2$ and PLi$_2$, Ground and Low-Lying Excited States

Demeter Tzeli, Aristotle Papakondylis, and Aristides Mavridis*

Laboratory of Physical Chemistry, Department of Chemistry, National and Kapodistrian University of Athens, P.O. Box 64004, 15710 Zografou, Athens, Greece

The ground states of the isovalent molecules NLi$_2$ ($\tilde{X}^2\Pi_u$) and PLi$_2$ ($\tilde{X}^2B_1$), along with some low-lying excited states ($^2B_2$, $^4\Sigma_g^-$, $^2\Sigma_g^-$, $^4\Sigma_u^-$, $^2\Sigma_u^-$, and $^2A_1$), have been examined using ab initio CISD, CASSCF, and MRCI methods in conjunction with relatively large correlation consistent basis sets. We report total energies, geometries, binding energies, Mulliken charges, energy gaps, and for certain states, potential energy curves. All states examined are bound with respect to the ground-state atoms N or P(^{4}S) + 2Li(^{2}S), while the mean binding energies N−Li and P−Li of NLi$_2$ and PLi$_2$ are 42.5 and 40.2 kcal/mol, respectively.

1. Introduction

In the present report we examine via ab initio methods the electronic structure of the ground state and of some low-lying excited states of the isovalent molecules dilithium nitride (NLi$_2$) and dilithium phosphide (PLi$_2$). To the best of our knowledge there are no experimental or theoretical results in the literature for NLi$_2$. The PLi$_2$ system has been observed in the gas phase by Knudsen-effusion mass spectrometry,[1] along with other phosphorus-lithiated species. We are also aware of some, as yet unpublished, ab initio results by Kudo[2] on the ground states of PLi and PLi$_2$ molecules (vide infra). On the other hand, experimental results on lithiated N- and P-species in the solid state have existed for quite a few years.[3] The interest in these systems is due to their ionic nature and the role they could potentially play as solid-state ionic conductors.

Using SCF, CISD(+corrections), CASSCF (complete active space SCF), CASSCF+1+2 (CASSCF + single + double replacements = MRCI), and MRCI+corrections methods in conjuction with rather large correlation consistent basis sets, we have examined the ground states $\tilde{X}^2\Pi_u$(NLi$_2$) and $\tilde{X}^2B_1$-(PLi$_2$), as well as the low-lying excited states $^2B_2$, $^2\Sigma_g^-$, $^2\Sigma_u^-$, $^2A_1$, $^4\Sigma_g^-$, and $^4\Sigma_u^-$ for both title molecules. In an effort to better understand the nature of the chemical bond in these unusual species, we have also constructed potential energy curves (PECs) for certain states; in particular for the ground $^2\Pi_u$ state of NLi$_2$ we constructed PECs referring to both dissociation channels, NLi$_2$ → NLi + Li and NLi$_2$ → N + 2Li.

The present report is a continuation of our work on lithiated species;[4] we believe that the simplicity of the Li atom (one active electron), in parallel with its low-lying first excited state ($\Delta E(^2P\leftarrow^2S)$ = 1.85 eV), presents an ideal case for the study of the chemical bond.

2. Basis Sets and Methods

For all atoms, the correlation consistent polarized basis sets of Dunning were used, cc-pVnZ, where n is a cardinal number characterizing the basis set quality.[5,6] One of the nicest properties of the cc-bases is their potential of improving in a well-defined and systematic way the quality of calculation and their convergence toward the "complete basis set" limits of various molecular properties within the methodology employed.[7]

For the N and P atoms the quadruple n = 4 (QZ) quality basis was employed but with the functions of g-symmetry removed (cc-pVQZ-g). For the N atom only and in conjuction with the CISD method, the augmented cc-pVQZ-g (cc-pVQZ + one diffuse function for each symmetry present = aug-cc-pVQZ-g) was used. For the Li atom the n = 3(TZ) basis was selected. For instance, the PLi$_2$ basis set reads as follows: (16s11p3d2f/(11s5p2d1f)$_2$) → [6s5p3d2f/(4s3p2d1f)$_2$], comprised of 110 contracted spherical Gaussians (i.e., five d and seven f functions). The reason for selecting these particular bases, e.g., n = 4 for the N and P atoms and n = 3 for the Li atom, will be discussed further in the next section.

As was already mentioned, the theoretical methodologies employed are SCF, CISD(SCF+1+2), CASSCF, and CASSCF+1+2 (MRCI). In the CASSCF calculations, the Li 2s-, N 2s2p-, and P 3s3p-like orbitals were included in the active space. The Li 1s-, N 1s-, and P 1s2s2p-like orbitals were optimized but always constrained to be doubly occupied. Given those restrictions, our CASSCF space for the triatomic species contains seven active orbitals and seven (valence) electrons. Depending on the symmetry of the state, the size of the CAS space ranges from 112 ($^4\Sigma_g^-$) to 404 ($^2A_1$) CSFs, with 988 665 and 1 501 544 CSFs, respectively, in the MRCI space. No corrections for basis set superposition errors were applied, assuming that the size of the basis sets was large enough. It should also be mentioned that the size extensivity error in all MRCI PECs studied was less than 0.1 mhartree.

Our computations were performed with the COLUMBUS[8] suite, with some CISD results checked by the MELD[9] code. Also, the MOLPRO[10,11] code was used for certain calculations on the diatomic molecule NLi.

3. Results and Discussion

a. The Diatomics NLi and PLi. Recently we have reported on the ground and low-lying states of NLi[4b] and PLi[4a] molecules. With the purpose of selecting basis sets of adequate size for the triatomic species NLi$_2$ and PLi$_2$, while at the same time keeping our calculations manageable, we have reexamined the dissociation energies (D_e) and bond lengths (r_e) of NLi and PLi ground states as a function of basis set size. Our results at the MRCI level, along with literature results, are reported in Table 1. Considering the D_e and r_e as the most sensitive parameters

TABLE 1: MRCI Results on the Ground X³Σ⁻ State of NLi and PLi as a Function of Basis Set Size: Energies (hartrees), Bond Distances r_e (angstroms), Dissociation Energies D_e (kcal/mol), and Harmonic Frequencies ω_e (cm⁻¹)

basis set	$-E$	r_e	D_e	ω_e
	NLi			
aug-cc-pVTZ/DZ[a]	61.98909	1.921	29.5	619.9
cc-pVQZ-g/cc-pVTZ	62.00663	1.885	33.3	655.2
cc-pVQZ/cc-pVTZ[b]	62.00774	1.879	33.5	663.2
cc-pVQZ-g/cc-pVQZ-g	62.00786	1.881	34.1	660.1
aug-cc-pVQZ-g/cc-pVTZ	62.00884	1.889	34.5	649.9
cc-pV5Z/cc-pVQZ[b]	62.01347	1.877	35.4	665.3
aug-cc-pV5Z/cc-pVQZ[b]	62.01451	1.879	35.8	662.2
DZ+P-Slater functions[c]	61.7781	1.85	19.6	657
6-311+G(2df)//6-31+G*[d]	d	1.874[e]	34.4[d]	681[e]
	PLi			
cc-pVQZ-g/cc-pVTZ	348.31423	2.357	36.3	476.8
cc-pVQZ-g/cc-pVQZ-g[f]	348.31497	2.351	36.8	479.1
aug-cc-pVQZ-g/cc-pVQZ-g	348.31554	2.353	37.1	478.7
6-311+G(2df)[g]	348.30484	2.342	38.4	495[h]
[5s4p2d/4s3p2d][i]	348.29936	2.372		

[a] Reference 4b. [b] Internally contracted MRCI, MOLPRO code. [c] Reference 12, CISD with respect to a two-configuration reference. [d] Reference 13a, QCISD(T), 6-311+G(2df)//MP2(full/6-31+G*), no absolute energy value is given. [e] Reference 13a, MP2(full)/6-311+G*. [f] Reference 4a. [g] Reference 13b, QCISD(T). [h] Reference 13b, MP2(full)/6-31+G*. [i] Reference 2, MRCI+Full-CI Davidson correction, contracted ANO-basis set (17s12p5d4f/14s9p4d3f) → [5s4p2d/4s3p2d].

with respect to the basis set size, Table 1 reveals that for NLi our best results, D_e = 35.8 kcal/mol and r_e = 1.879 Å, are in fair agreement with the cc-pVQZ-g/cc-pVTZ numbers, that is, D_e = 33.3 kcal/mol and r_e = 1.884 Å. Incidentally, the D_e value of NLi in the aug-cc-pV5Z/cc-pVQZ basis is the most accurate reported so far in the literature.

Similarly, results on the PLi molecule are presented in Table 1, from where it is obvious that the cc-pVQZ-g/cc-pVTZ numbers are in good agreement with the more flexible basis sets.

The above results rationalize our selection of the QZ-g/TZ basis in the treatment of both triatomic species, NLi₂ and PLi₂.

Table 2 summarizes all relevant arithmetic results on NLi and PLi for the ground X³Σ⁻ and the first excited A³Π states in the QZ-g/TZ basis, using different methodologies. Analysis of similar results with that of Table 2 (with a smaller and slightly larger basis set for NLi and PLi, respectively) and binding mechanisms can be found elsewhere.[4a,b] The only purpose of presenting Table 2 is its relevance in discussing the triatomics NLi₂ and PLi₂. A few comments though are in order. Both molecules in both states are ionic with almost half an electron transferred from Li to N or P in the X³Σ⁻ state(s); in the X³Σ⁻ state(s) there is a single bond of σ-character, while in the A³Π state(s) the atoms are held together by a π-bond, a half σ-bond, and a half π-bond (by a half-bond we mean that only one electron is involved in the bonding process). It should also be mentioned that the A³Π state correlates to N(⁴S) + Li(²P) or P(²D) + Li(²S) fragments. This double-bond character of the A³Π state(s) is reflected in the impressive bond length shortening along with a significant increase in the D_e values (with respect to the asymptotic products) as compared to the X³Σ⁻ state, Table 2.

b. The Triatomics NLi₂ and PLi₂. Tables 3 and 4 present numerical results on NLi₂ and PLi₂, respectively; we report total energies, equilibrium geometries, dissociation energies with respect to the ground-state fragments N or P (⁴S) + 2Li(²S), Mulliken charges, and energy gaps of the ground and some low-lying excited states and in different methodologies. In what

TABLE 2: Absolute Energies E (hartrees), Bond Lengths r_e (angstroms), Dissociation Energies D_e (kcal/mol), Mulliken Charges q (N or P), and Energy Differences T_e (kcal/mol) of NLi and PLi in the X³Σ⁻ and A³Π States

method	$-E$	r_e	$D_e{}^c$	q	T_e
	NLi(X³Σ⁻)				
SCF	61.833 53	1.844	0.4	−0.54	
CISD	62.001 73	1.873	30.9	−0.55	
CISD+Q[a]	62.013	1.886	35		
CASSCF	61.868 89	1.900	15.5	−0.51	
MRCI	62.006 63	1.885	33.3	−0.50	
MRCI+Q[b]	62.014	1.890	35		
	NLi(A³Π)				
CASSCF	61.862 95	1.734	54.2	−0.40	3.7
MRCI	61.998 25	1.737	70.5	−0.41	5.3
MRCI+Q[b]	62.005	1.740	72		5.4
	PLi(X³Σ⁻)				
SCF	348.173 80	2.342	14.3	−0.45	
CISD	348.308 77	2.339	34.0	−0.43	
CISD+Q[a]	348.320	2.344	37		
CASSCF	348.198 88	2.400	21.3	−0.39	
MRCI	348.314 23	2.357	36.3	−0.41	
MRCI+Q[b]	348.323	2.356	38		
	PLi(A³Π)				
CASSCF	348.180 67	2.219	40.0	−0.40	11.4
MRCI	348.292 46	2.227	56.9	−0.34	13.7
MRCI+Q[b]	348.301	2.231	59		14.1

[a] Single-reference Davidson correction for unlinked quadruples. [b] Multireference Davidson correction, ref 14. [c] X³Σ⁻, D_e with respect to the ground-state products. A³Π, D_e with respect to asymptotic products, i.e., NLi(A³Π) → N(⁴S) + Li(²P) and PLi(A³Π) → P(²D) + Li(²S).

follows we analyze our findings with an emphasis on the binding mechanisms.

NLi₂, Ground $\tilde{X}^2\Pi_u$ ($1\sigma_g^2 2\sigma_g^2 1\sigma_u^2 3\sigma_g^2 2\sigma_u^2 1\pi_u^3$) State. We imagine that the molecule is formed either by a ground-state Li(²S) atom approaching the first excited A³Π state of NLi or by a Li atom in its excited ²P state approaching the ground X³Σ⁻ of NLi. A clear visualization of these two routes is obtained by using valence bond−Lewis icons. Of course, at equilibrium,
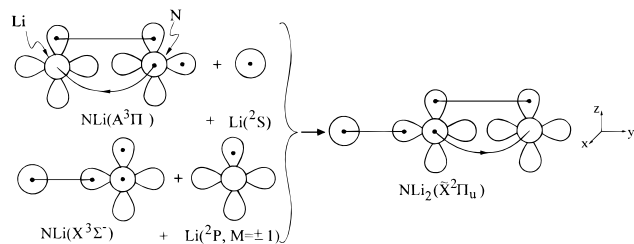
both the above molecular picture and its mirror image are present, so the two Li atoms are strictly equivalent. At equilibrium the CAS atomic populations are

$$\text{N:}\quad 2s^{1.73}2p_x^{0.88}2p_y^{1.37}2p_z^{1.44}$$

$$\text{Li:}\quad 2s^{0.22}2p_x^{0.04}2p_y^{0.11}2p_z^{0.31}$$

in reasonable agreement with the above picture. Each Li atom is losing 0.66 e⁻ via the σ-frame gaining at the same time 0.35 e⁻ via the π-frame; overall, ∼0.4 e⁻ are transferred to the N atom. Bending the molecule results in the two nondegenerate components (Renner−Teller splitting) $^2B_1(3a_1^2 4a_1^2 1b_1^1 2b_2^2)$ and $^2A_1(3a_1^2 4a_1^1 1b_1^2 2b_2^2)$, degenerate in the linear $|\Lambda|$ = 1 geometry, Figure 1. We observe that NLi₂ is a very floppy molecule, requiring just 0.6 mhartree to bend it up to 140° on the $^2B_1$ surface.

Electronic Structure of NLi₂ and PLi₂

J. Phys. Chem. A, Vol. 102, No. 12, 1998 **2225**

TABLE 3: Absolute Energies E (hartrees), Bond Lengths r_e (angstroms), Angles θ (degrees $\angle$LiNLi), Binding Energies D_e (kcal/mol), Mulliken Charges q_N, and Energy Differences T_e (kcal/mol) of the Ground $^2\Pi_u$ State and Some Low-Lying Excited States of NLi₂

method	$-E$	r_e	θ	$D_e{}^a$	q	$T_e{}^b$
			$\tilde{X}^2\Pi_u$			
SCF	69.290 85	1.746	180.0	15.9	−0.57	
CISD	69.505 84	1.767	180.0	75.5	−0.58	
CISD+Q^c	69.523	1.777	180.0	83		
CASSCF	69.375 71	1.790	180.0	62.0	−0.43	
MRCI	69.521 59	1.782	180.0	84.9	−0.45	
MRCI+Q^d	69.530	1.786	180.0	88		
			$^2B_2$			
SCF	69.268 38	1.671	140.2	1.8	−0.50	14.1
CISD	69.487 24	1.702	125.8	63.8	−0.47	11.7
CISD+Q^c	69.506	1.715	123.2	73		10.8
CASSCF	69.361 01	1.722	118.4	52.8	−0.41	9.2
MRCI	69.506 15	1.738	111.4	75.3	−0.45	9.7
MRCI+Q^d	69.515	1.750	106.4	78		9.9
			$^2\Sigma_u{}^{+\ e}$			
SCF	69.267 93	1.660	180.0		−0.53	14.4
CISD	69.484 62	1.678	180.0		−0.53	13.3
CISD+Q^c	69.502	1.686	180.0			13.1
CASSCF	69.358 55	1.684	180.0		−0.32	10.8
MRCI	69.502 57	1.689	180.0		−0.35	11.9
MRCI+Q^d	69.510	1.693	180.0			12.6
			$^4\Sigma_g{}^-$			
SCF	69.307 62	1.925	180.0	26.4	−0.37	−10.5
CISD	69.478 53	1.912	180.0	58.3	−0.33	17.1
CISD+Q^c	69.489	1.921	180.0	62		21.5
CASSCF	69.342 27	1.930	180.0	41.0	−0.34	21.0
MRCI	69.483 93	1.921	180.0	61.3	−0.32	23.6
MRCI+Q^d	69.492	1.925	180.0	64		24.2
			$^2\Sigma_g{}^-$			
SCF	69.304 03	1.895	180.0	24.1	−0.40	−8.3
CISD	69.474 38	1.924	180.0	55.7	−0.36	19.7
CISD+Q^c	69.485	1.933	180.0	59		24.1
CASSCF	69.339 08	1.943	180.0	39.0	−0.35	23.0
MRCI	69.478 56	1.928	180.0	57.9	−0.35	27.0
MRCI+Q^d	69.486	1.931	180.0	60		27.9
			$^4\Sigma_u{}^-$			
SCF	69.296 84	1.908	180.0	19.6	−0.28	−3.8
CISD	69.466 03	1.930	180.0	50.5	−0.28	25.0
CISD+Q^c	69.476	1.938	180.0	54		29.6
CASSCF	69.332 05	1.946	180.0	34.6	−0.36	27.4
MRCI	69.471 50	1.940	180.0	53.5	−0.36	31.4
MRCI+Q^d	69.479	1.944	180.0	56		32.4
			$^2\Sigma_u{}^-$			
SCF	69.295 78	1.908	180.0	18.9	−0.28	−3.1
CISD	69.464 67	1.929	180.0	49.6	−0.26	25.8
CISD+Q^c	69.474	1.936	180.0	53		31
CASSCF	69.330 68	1.943	180.0	33.7	−0.37	28.3
MRCI	69.470 00	1.936	180.0	52.6	−0.36	32.4
MRCI+Q^d	69.477	1.939	180.0	55		33
			$^2A_1$			
SCF	69.229 21	1.937	89.1	−22.8	−0.24	38.7
CISD	69.418 40	1.954	88.4	20.6	−0.24	54.9
CISD+Q^c	69.434	1.962	88.4	28		55.9
CASSCF	69.304 24	1.978	86.4	17.1	−0.32	44.9
MRCI	69.428 88	1.963	87.9	26.8	−0.34	58.2
MRCI+Q^d	69.440	1.954	89.3	31		56.8

^{a} With respect to the ground-state products N(^{4}S) + 2Li(^{2}S). ^{b} With respect to the ground $\tilde{X}^2\Pi_u$ state. ^{c} Single-reference Davidson correction for unlinked quadruples. ^{d} Multireference Davidson correction, ref 14. ^{e} Obtained from the $^2B_2$ state in the limit of $\theta = 180.0°$.

Now, there are two ways of taking the molecule apart: one by simultaneously stretching away the two Li atoms in a symmetric fashion maintaining the center of symmetry; the second by stretching away one Li atom with respect to the NLi fragment. The potential energy curves of these two modes of
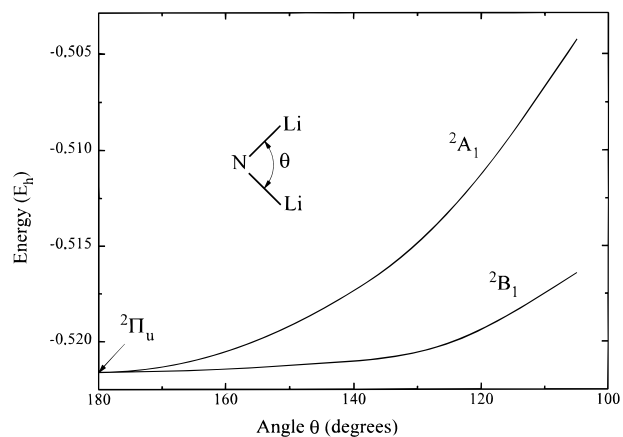

Figure 1. Splitting of the NLi₂ (linear) $\tilde{X}^2\Pi_u$ state as a function of the θ angle, MRCI level of theory.
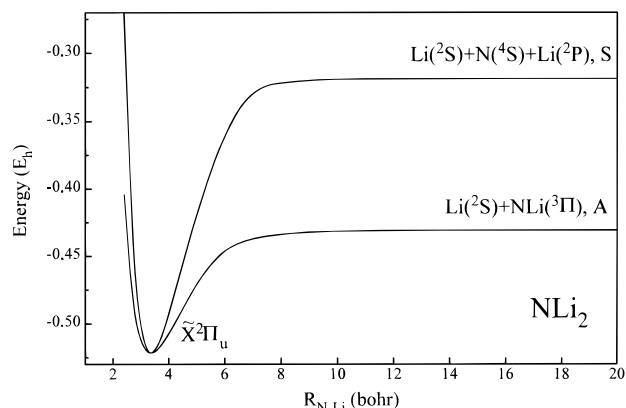
Figure 2. Symmetric (S) and asymmetric (A) PECs of NLi₂ in the linear $^2\Pi_u$ configuration, MRCI level of theory.

opening, symmetric (S) and asymmetric (A), are shown in Figure 2 with corresponding numerical results presented in Table 5. Both PECs were obtained by defining the z-axis to be the molecular axis. As we can see from Figure 2, the S-opening traces its lineage to one Li atom in the ground ^{2}S state and the other to the first excited ^{2}P state

$$NLi_2(\tilde{X}^2\Pi_u) \rightarrow Li(^2S) + Li(^2P) + N(^4S)$$
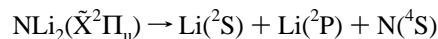
as it should. The atomization energy of the above process is 127.4 kcal/mol with respect to the ^{2}P state of Li (Table 5) or 84.9 kcal/mol with respect to the ground-state products (Table 3), at the MRCI level of theory. Therefore the mean dissociation N−Li energy is 84.9/2 = 42.5 kcal/mol, about 10 kcal/mol larger than the D_e of NLi ($X^3\Sigma^-$), Table 2.

The A-opening mode correlates to the first excited A$^3\Pi$ state of NLi and the ground ^{2}S state of the Li atom

$$NLi_2(\tilde{X}^2\Pi_u) \rightarrow NLi(A^3\Pi) + Li(^2S)$$

(Figure 2) again as it should. The D_e of this process with respect to the asymptotic products (internal bond strength) is 57.1 kcal/mol at the MRCI level (Table 5) or 57.1−5.3 = 51.8 kcal/mol (Table 2) with respect to the ground-state products, NLi ($X^3\Sigma^-$) + Li(^{2}S). Both the S- and A-opening modes are in agreement with the binding mechanism of NLi₂ presented before.

PLi₂, Ground $\tilde{X}^2B_1$ ($5a_1{}^2 6a_1{}^2 3b_2{}^2 2b_1{}^1$) State. The single most important difference between the ground states of NLi₂ and PLi₂ molecules is that the former is linear while the latter is strongly bent, $\theta = 100°$ at the MRCI level (Table 4,

TABLE 4: Absolute Energies E (hartrees), Bond Lengths r_e (angstroms), Angles θ (degrees $\angle$LiPLi), Binding Energies D_e (kcal/mol), Mulliken Charges q_P, and Energy Differences T_e (kcal/mol) of the Ground $\tilde{X}^2B_1$ State and Some Low-Lying Excited States of PLi$_2$

method	$-E$	r_e	θ	$D_e{}^a$	q	$T_e{}^b$	method	$-E$	r_e	θ	$D_e{}^a$	q	$T_e{}^b$
		$\tilde{X}^2B_1$							$^2\Sigma_g{}^-$				
SCF	355.639 49	2.264	116.6	35.0	−0.51		SCF	355.618 90	2.439	180.0	22.1	−0.25	12.9
CISD	355.803 54	2.264	114.2	72.9	−0.49		CISD	355.756 14	2.439	180.0	43.2	−0.24	29.8
CISD+Q^c	355.820	2.272	111.2	79			CISD+Q^c	355.768	2.445	180.0	46		32.5
CASSCF	355.685 35	2.297	102.0	55.1	−0.52		CASSCF	355.642 97	2.473	180.0	28.5	−0.23	26.6
MRCI	355.817 36	2.291	100.0	80.4	−0.47		MRCI	355.761 93	2.450	180.0	45.8	−0.24	34.8
MRCI+Q^d	355.829	2.297	98.3	84			MRCI+Q^d	355.772	2.454	180.0	48		36.0
MRCI+Q^e	355.801 14	2.267	112.0										
		$^2\Pi_u{}^f$							$^4\Sigma_u{}^-$				
							SCF	355.609 07	2.431	180.0	15.9	−0.28	19.1
SCF	355.638 59	2.231	180.0	34.4	−0.51	0.6	CISD	355.748 82	2.424	180.0	38.6	−0.26	34.3
CISD	355.802 75	2.229	180.0	72.4	−0.50	0.5	CISD+Q^c	355.761	2.429	180.0	42		36.9
CISD+Q^c	355.819	2.232	180.0	78.2		0.8	CASSCF	355.640 04	2.418	180.0	26.7	−0.26	28.4
CASSCF	355.681 22	2.225	180.0	52.5	−0.53	2.6	MRCI	355.755 59	2.425	180.0	41.8	−0.25	38.8
MRCI	355.813 49	2.230	180.0	78.1	−0.50	2.4	MRCI+Q^d	355.765	2.432	180.0	44		40.4
MRCI+Q^d	355.825	2.234	180.0	82		2.6			$^2\Sigma_u{}^-$				
		$^2B_2$					SCF	355.607 56	2.425	180.0	15.0	−0.29	20.0
SCF	355.614 02	2.256	83.6	19.0	−0.55	16.0	CISD	355.747 27	2.421	180.0	37.6	−0.27	35.3
CISD	355.783 03	2.261	82.4	60.1	−0.50	12.9	CISD+Q^c	355.759	2.425	180.0	41		38.0
CISD+Q^c	355.801	2.272	81.3	67		11.7	CASSCF	355.638 77	2.418	180.0	25.9	−0.28	29.2
CASSCF	355.666 95	2.296	76.7	43.6	−0.45	11.6	MRCI	355.754 03	2.422	180.0	40.8	−0.26	39.7
MRCI	355.798 38	2.286	78.2	68.7	−0.47	11.9	MRCI+Q^d	355.763	2.426	180.0	43		41.5
MRCI+Q^d	355.810	2.288	78.3	72		12.1			$^2A_1$				
		$^2\Sigma_u{}^+{}^g$					SCF	355.581 58	2.497	66.9	−1.3	−0.29	36.3
SCF	355.592 13	2.177	180.0		−0.56	29.7	CISD	355.734 54	2.489	67.4	29.6	−0.28	43.3
CISD	355.760 52	2.170	180.0		−0.53	27.0	CISD+Q^c	355.751	2.490	67.4	36		43.1
CISD+Q^c	355.778	2.173	180.0			26.5	CASSCF	355.620 61	2.508	66.1	14.5	−0.26	40.6
CASSCF	355.644 02	2.151	180.0		−0.54	25.9	MRCI	355.743 59	2.486	67.3	34.3	−0.24	46.3
MRCI	355.773 24	2.166	180.0		−0.52	27.7	MRCI+Q^d	355.758	2.489	67.4	40		44.9
MRCI+Q^d	355.784	2.172	180.0			28.4							
		$^4\Sigma_g{}^-$											
SCF	355.619 37	2.429	180.0	22.4	−0.24	12.6							
CISD	355.761 32	2.427	180.0	46.4	−0.21	26.5							
CISD+Q^c	355.774	2.433	180.0	50		28.7							
CASSCF	355.649 59	2.419	180.0	32.7	−0.23	22.4							
MRCI	355.768 17	2.427	180.0	49.7	−0.21	30.9							
MRCI+Q^d	355.778	2.435	180.0	52.5		32.0							

^{a} With respect to the ground-state products P(^{4}S) + 2Li(^{2}S). ^{b} With respect to the ground $\tilde{X}^2B_1$ state. ^{c} Single-reference Davidson correction for unlinked quadruples. ^{d} Multireference Davidson correction, ref 14. ^{e} Reference 2. ANO-basis set, (17s12p5d4f/(14s9p4d3f)$_2$) → [5s4p2d/(4s3p2d)$_2$]. MRCI+Full CI Davidson correction. ^{f} Obtained from the $\tilde{X}^2B_1$ state in the limit of $\theta = 180.0°$, $\tilde{X}^2B_1 \rightarrow {}^2\Pi_u(^2B_1,^2A_1)$. ^{g} Obtained from the $^2B_2$ state in the limit of $\theta = 180.0°$.

TABLE 5: Dissociation Energies D_e (kcal/mol) with Respect to Asymptotic Fragments of NLi$_2$ ($\tilde{X}^2\Pi_u$) and PLi$_2$ ($\tilde{X}^2B_1$, $^2\Pi_u$)

	NLi$_2$		PLi$_2$		
	$\tilde{X}^2\Pi_u$		$^2\Pi_u$		$\tilde{X}^2B_1$
method	D_e-A^a	D_e-S^b	D_e-A^c	D_e-S^d	D_e-S^e
CASSCF	50.5	104.5	42.6	82.6	55.1
MRCI	57.1	127.4	55.4	112.3	80.4
MRCI+Q^f	58	131	57.4	117	84

^{a} Asymmetric opening, NLi$_2$($\tilde{X}^2\Pi_u$) → NLi(A$^3\Pi$) + Li(^{2}S). ^{b} Symmetric opening, NLi$_2$($\tilde{X}^2\Pi_u$) → Li(^{2}S) + Li(^{2}P) + N(^{4}S). ^{c} Asymmetric opening, PLi$_2$($^2\Pi_u$) → PLi(A$^3\Pi$) + Li(^{2}S). ^{d} Symmetric opening, PLi$_2$($^2\Pi_u$) → 2Li(^{2}S) + P(^{2}D). ^{e} Angular symmetric opening, PLi$_2$($\tilde{X}^2B_1$) → 2Li(^{2}S) + P(^{4}S). ^{f} Multireference Davidson correction, ref 14.

Figure 3). In the linear $^2\Pi_u$ configuration exactly the same binding mechanism operates as in NLi$_2$, with the one in situ Li atom in the ^{2}P state and the other in the ground ^{2}S state as described before. As we bend the molecule in a $^2B_1$ fashion, the total energy falls very slowly till it reaches a minimum at $\theta = 100°$, with an energy gaining (inversion barrier) of 2.4 kcal/mol at equilibrium (Table 4, Figure 3). Despite the very small energy difference between the bent and the linear geometries

(the molecule in essence is quasilinear), PLi$_2$ is predicted to be formally bent at all levels of theory, even at the SCF (Table 4). Figure 3 presents the $^2\Pi_u \rightarrow {}^2B_1$ PEC along with the $^2\Pi_u \rightarrow {}^2A_1$ PEC. Certainly in the $\tilde{X}^2B_1$ state the binding appears to be quite different from that in the linear $^2\Pi_u$ case, the prevailing valence bond−Lewis icon in this state being i.e., two σ-bonds


PLi$_2$($\tilde{X}^2B_1$)
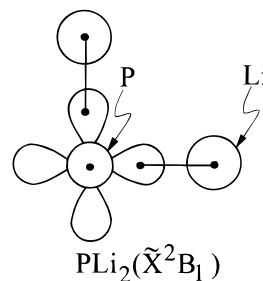
originating from the ground state of P and Li atoms, assisted with small promotions to the Li p$_y$- and p$_z$-orbitals. From Table 4 we also observe a significant bond length difference between the bent and the linear configurations, the latter being shorter by 0.06 Å, reflecting the different bonding character between the two cases, bent vs linear.
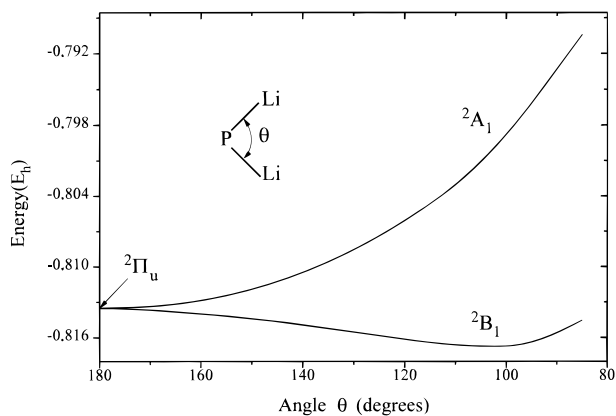
Figure 3. Splitting of the PLi$_2$ (linear) $^2\Pi_u$ state as a function of the θ angle, MRCI level of theory.
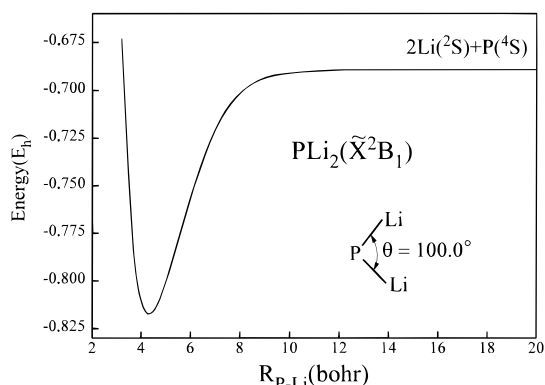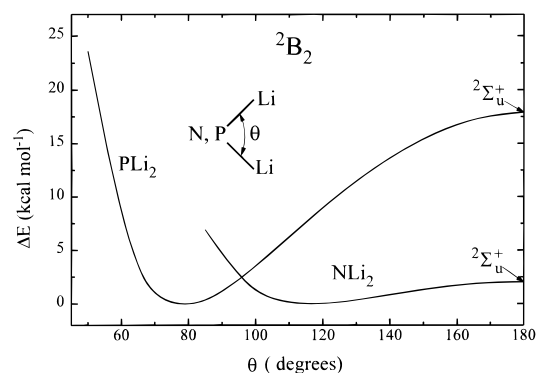

Figure 4. Potential energy curve of PLi$_2$ in the $\tilde{X}^2B_1$ ($\theta = 100°$), MRCI level of theory.
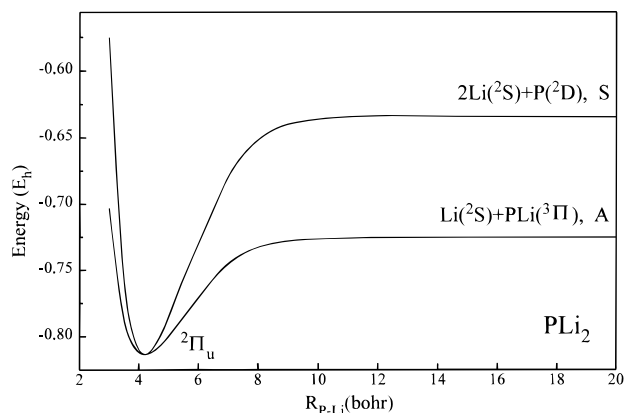
Figure 5. Symmetric (S) and asymmetric (A) PECs of PLi$_2$ ($^2\Pi_u$ at $\theta = 180°$), MRCI level of theory.

Now, as we take the molecule apart in a symmetric fashion, maintaining the C_{2v} symmetry and a LiPLi angle of 100°, we end up with the ground-state fragments, $2\text{Li}(^2S) + \text{P}(^4S)$, obtaining a mean P–Li binding energy of 80.4/2 = 40.2 kcal/mol at the MRCI level (Table 5). The corresponding PEC, PLi$_2$ ($\tilde{X}^2B_1$) $\rightarrow 2\text{Li}(^2S) + \text{P}(^4S)$, $\theta = 100°$, is shown in Figure 4.

As in the NLi$_2$ case the PLi$_2$ in its linear $^2\Pi_u$ configuration ($^2B_1 \rightarrow {}^2\Pi_u$), can be thought as the result of either the PLi-(A$^3\Pi$) + Li(^2S) or the PLi(X$^3\Sigma^-$) + Li(^2P) process (vide supra). By pulling apart a Li atom, i.e., breaking a PLi–Li bond (A-mode), the PEC of Figure 5 is obtained, with products PLi-(A$^3\Pi$) + Li(^2S). This is of course expected because the A$^3\Pi$ ← X$^3\Sigma^-$ energy difference of PLi is smaller than the ^2P ← ^2S energy difference of the Li atom, 13.7 kcal/mol (Table 2) vs 42.5 kcal/mol, respectively. The resulting PLi–Li D_e with

respect to the ground-state fragments PLi(A$^3\Sigma^-$) + Li(^2S) is 55.4−13.7 = 41.7 kcal/mol (Table 5, MRCI level). Correcting this value for the opening ($\tilde{X}^2B_1 \rightarrow {}^2\Pi_u$) energy loss of 2.4 kcal/mol (Table 4), the PLi–Li binding energy D_e is 44.1 kcal/mol. By pulling the molecule apart in an S-fashion (linearly), PLi$_2$ $\rightarrow$ 2Li + P, the PEC of Figure 5 is obtained with end fragments $2\text{Li}(^2S) + \text{P}(^2D)$. Here the situation differs from the corresponding NLi$_2$ case (Figure 2), where the end products are Li-(^2S) + Li(^2P) + N(^4S), due to an avoided crossing between the Li(^2S) + Li(^2P) + P(^4S) and $2\text{Li}(^2S) + \text{P}(^2D)$ PECs: the ^2D state of the P atom is 8.2 kcal/mol (10.0 kcal/mol experimentally[15]), lower than the ^2P state of the Li atom.

Finally, PLi$_2$ is as ionic as NLi$_2$ ($^2\Pi_u$) in both its bent ($\tilde{X}^2B_1$) or linear ($^2\Pi_u$) geometry, with a total of ∼0.5 e$^-$ transferred to the P atom (Table 4).

NLi$_2$, PLi$_2$, $^2B_2$. The $^2B_2$ states of NLi$_2$ ($3a_1^2 4a_1^2 1b_1^2 2b_2^1$) and PLi$_2$ ($5a_1^2 6a_1^2 2b_1^2 3b_2^1$) species are 9.7 and 11.9 kcal/mol, respectively, above their ground states. Both are practically equally bound with respect to their ground-state atoms, with mean N–Li and P–Li binding energies of 37.7 and 34.4 kcal/mol (MRCI, Tables 3 and 4). However the LiPLi angle is 30° smaller than the LiNLi angle. In addition, NLi$_2$ is a floppy system having an inversion barrier of just 2.2 kcal/mol as compared to 17.2 kcal/mol of PLi$_2$ (MRCI). The PECs of the two systems as functions of θ, keeping the bond lengths constant at their equilibrium values, are shown in Figure 6 with both systems ending up in a $^2\Sigma_u^+$ symmetry. The valence bond–Lewis pictures of the binding scheme in the *linear* $^2\Sigma_u^+$ configuration is quite interesting with the in situ N or P atoms
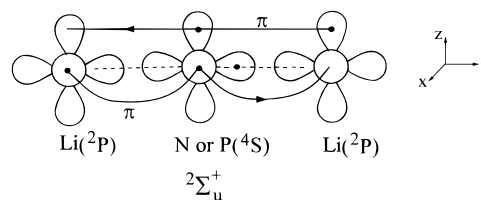
in the ground ^4S state and the in situ Li atoms in the excited ^2P state. The CAS atomic populations are clearly in support of the above picture as the main bonding scheme in the linear geometry

NLi$_2$: $2s^{1.69} 2p_x^{1.41} 2p_y^{0.82} 2p_z^{1.41} / 2s^{0.08} 2p_x^{0.22} 2p_y^{0.06} 2p_z^{0.30}$

PLi$_2$: $3s^{1.63} 3p_x^{1.61} 3p_y^{0.67} 3p_z^{1.60} / 2s^{0.15} 2p_x^{0.14} 2p_y^{0.07} 2p_z^{0.24}$

where the first entry refers to the N or P populations and the second to the Li populations. In other words, in the (linear)


Figure 6. Potential energy curves (relative energies) of NLi$_2$ and PLi$_2$ in the $^2B_2$ state(s) with respect to the θ angle, MRCI level of theory.

$^2\Sigma_u^+$ configuration the molecules are held together by two 3-center-2-electron π-bonds perpendicular to each other and a 3-center-1-electron σ-bond. This strong delocalization of the π-system is also the cause of the significant shortening of the bond lengths in the $^2\Sigma_u^+$ configurations, as compared to the $^2B_2$ states, by 0.05 and 0.11 Å for the NLi_2 and PLi_2, respectively (MRCI, Tables 3 and 4).

NLi_2, PLi_2, $^4\Sigma_g^-$($^4B_1$) $3\sigma_g^2 4\sigma_g^1 1\pi_u^2 2\sigma_u^2$ and $5\sigma_g^2 6\sigma_g^1 2\pi_u^2 3\sigma_u^2$ ($3a_1^2 4a_1^1 2b_2^2 5a_1^1 1b_1^1$, $5a_1^2 6a_1^1 3b_2^2 7a_1^1 2b_1^1$). We can imagine the formation of the $^4\Sigma_g^-$ state of either the NLi_2 or PLi_2 systems as taking place by the approach of a ground ^2S Li atom from infinity to the ground $X^3\Sigma^-$ state of NLi or PLi while coupling the three electrons into a quartet, $NLi(X^3\Sigma^-) + Li(^2S) \rightarrow NLi_2(^4\Sigma_g^-)$. The prevailing valence bond–Lewis icon gives a clear representation of the "bonding" interaction:
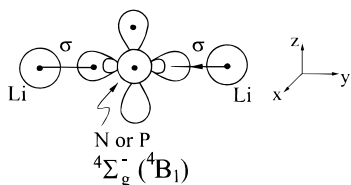
The symmetry of the system imposes the coexistence of the mirror image of the above icon in the equilibrium, so the two Li atoms are strictly equivalent with a 3-center-3-electron bond along the σ-frame (y-axis). The equilibrium CAS atomic populations are revealing:

NLi_2: $\quad 2s^{1.84} 2p_x^{0.96} 2p_y^{1.59} 2p_z^{0.96} / 2s^{0.59} 2p_x^{0.01} 2p_y^{0.09} 2p_z^{0.08}$

PLi_2: $\quad 3s^{1.79} 3p_x^{0.96} 3p_y^{1.51} 3p_z^{0.96} / 2s^{0.64} 2p_x^{0.01} 2p_y^{0.06} 2p_z^{0.09}$

Grossly 0.5 e$^-$ are transferred to the N or P atoms through the σ-frame with a concomitant $\sim$0.2 e$^-$ transfer from N or P atoms to the p_y, p_z atomic-like orbitals of the Li atoms.

This state is bound with respect to the ground-state atoms by 61.3 (NLi_2) and 49.7 (PLi_2) kcal/mol (MRCI, Tables 3 and 4) or mean binding energies, N–Li and P–Li of $\sim$31 and 25 kcal/mol, respectively. This nature of interaction dictates large bond lengths, and indeed we have for both molecules a bond lengthening of 0.14 Å as compared to the ground states (MRCI). It is remarkable that in the NLi_2 system and at the SCF level the $^4\Sigma_g^-$ state is *lower* in energy by 10.5 kcal/mol than the ground $\tilde{X}^2\Pi_u$ state. It is obvious that the SCF wave function gives a qualitatively correct description of this state, and of course we can even separate correctly one Li atom at the Hartree–Fock level. The PECs of $NLi_2(^4\Sigma_g^-) \rightarrow NLi(X^3\Sigma^-) + Li(^2S)$ and $PLi_2(^4\Sigma_g^-) \rightarrow PLi(X^3\Sigma^-) + Li(^2S)$ at the MRCI level are shown in Figures 7 and 8, with D_e values of 28.0 and 13.3 kcal/mol, respectively. These numbers should be contrasted with the mean D_e values previously reported of 31 and 25 kcal/mol.

NLi_2, PLi_2, $^4\Sigma_u^-$, ($^4A_2$; $3a_1^2 4a_1^1 2b_2^2 3b_2^1 1b_1^1$, $5a_1^2 6a_1^1 3b_2^2 4b_2^1 2b_1^1$). By alloting the $5a_1(4\sigma_g)$ electron of the NLi_2 $^4\Sigma_g^-$ state to a $3b_2(3\sigma_u)$ symmetry orbital, the $^4\Sigma_u^-$ state is obtained, i.e., $3\sigma_g^2 1\pi_u^2 2\sigma_u^2 3\sigma_u^1$. Mutatis mutandis the same is true for the PLi_2 system. As a result the $^4\Sigma_u^-$ state for both molecules is similar in every respect to the $^4\Sigma_g^-$ state: bond lengths, bonding character, ionicity, and CAS populations are practically the same between the two states. The only difference between the $^4\Sigma_u^-$ and the $^4\Sigma_g^-$ states is that the former has a $\sim$8
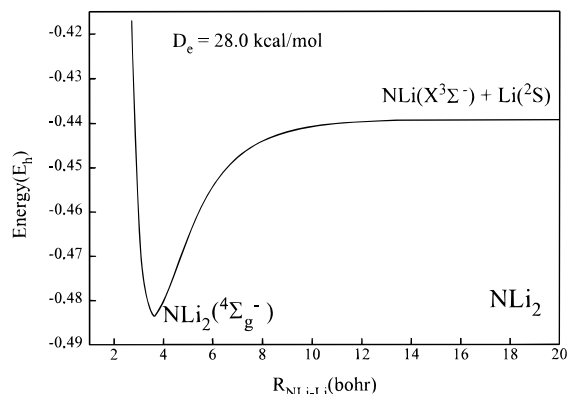

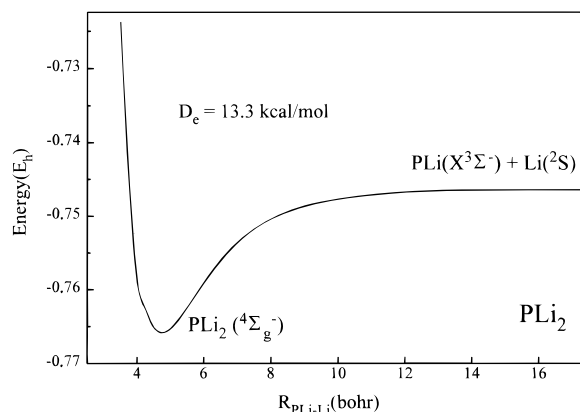**Figure 7.** MRCI PEC of the NLi–Li bond-breaking process, $^4\Sigma_g^-$ state.

Figure 8. MRCI PEC of the PLi–Li bond-breaking process, $^4\Sigma_g^-$ state.

kcal/mol smaller binding energy (atomization energy) with respect to the ground-state atoms (MRCI, Tables 3, 4), for both molecular systems.

NLi_2, PLi_2, $^2\Sigma_g^-$($^2A_2$). In both molecules the bonding originates from the first excited $^2D(M=0)$ state of N or P. The calculated MRCI level energy differences $\Delta E(^2D \leftarrow ^4S)$ for the N and P atoms are 2.457 and 1.484 eV, respectively, with corresponding experimental values of 2.384 and 1.410 eV.[15] The valence bond–Lewis cartoon representing the main features of binding is
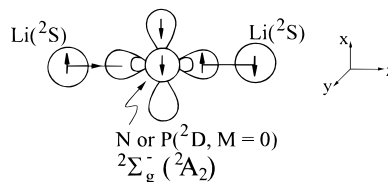
The situation differs from the $^4\Sigma_g^-$ state of NLi_2 or PLi_2 by one spin-flip on the N or P atoms, resulting in a more complicated description of the leading configuration. At the CASSCF level the leading configurations of NLi_2 and PLi_2 have the following electron allocations (notice that the molecular axis is the z-axis):

NLi_2: $\quad ^2\Sigma_g^-(^2A_2) = 1/6^{1/2}[(4a_1)^2 (5a_1)^2 (1b_1)^1 (1b_2)^1 (6a_1)^1]$
$$(2\alpha\alpha\beta - \alpha\beta\alpha - \beta\alpha\alpha)$$

PLi_2: $\quad ^2\Sigma_g^-(^2A_2) = 1/6^{1/2}[(6a_1)^2 (7a_1)^2 (2b_1)^1 (2b_2)^1 (8a_1)^1]$
$$(2\alpha\alpha\beta - \alpha\beta\alpha - \beta\alpha\alpha)$$

The equilibrium CAS atomic populations are

NLi$_2$: $2s^{1.84}2p_x^{0.96}2p_y^{0.96}2p_z^{1.58}/2s^{0.55}2p_x^{0.01}2p_y^{0.01}2p_z^{0.21}$

PLi$_2$: $3s^{1.79}3p_x^{0.97}3p_y^{0.97}3p_z^{1.44}/2s^{0.60}2p_x^{0.0}2p_y^{0.0}2p_z^{0.25}$

corroborating the previous given icon. Clearly, the π p$_{x,y}$ electrons of N or P atoms remain intact, while the 3-electron-3-center σ-bond is assisted by transfer of ~0.4 e$^-$ via the σ-frame from the Li atoms to the N or P atoms. From Tables 3 and 4 the similarity between the $^4\Sigma_g^-$ and $^2\Sigma_g^-$ states is clear: for both molecules the D_e values with respect to the ground-state products of the $^2\Sigma_g^-$ state are smaller by less than 4 kcal/mol than the D_e values of the $^4\Sigma_g^-$ state, while the bond distances lengthen by only approximately 0.01 and 0.02 Å in NLi$_2$ and PLi$_2$, respectively, as compared to the $^4\Sigma_g^-$ state.

NLi$_2$, PLi$_2$, $^2\Sigma_u^-$(^{2}A$_2$). The situation here is very similar to the previously discussed $^2\Sigma_g^-$ state. The same valence bond−Lewis icon describes the binding scheme, but this time the *y*-axis is the molecular axis with *z* being the 2-fold axis. The leading configurations of the CASSCF wave functions are

NLi$_2$: $^2\Sigma_u^-(^2A_2) = 1/6^{1/2}[(3a_1)^2(4a_1)^1(2b_2)^2(1b_1)^1(3b_2)^1]$

$(2\alpha\alpha\beta-\alpha\beta\alpha-\beta\alpha\alpha)$

PLi$_2$: $^2\Sigma_u^-(^2A_2) = 1/6^{1/2}[(5a_1)^2(6a_1)^1(3b_2)^2(2b_1)^1(4\,b_2)^1]$

$(2\alpha\alpha\beta-\alpha\beta\alpha-\beta\alpha\alpha)$

The equilibrium CAS atomic populations are practically the same as those of the $^2\Sigma_g^-$ state for both molecules (remember that *y* is the molecular axis)

NLi$_2$: $2s^{1.84}2p_x^{0.96}2p_y^{1.60}2p_z^{0.96}/2s^{0.36}2p_x^{0.01}2p_y^{0.28}2p_z^{0.05}$

PLi$_2$: $3s^{1.81}3p_x^{0.97}3p_y^{1.49}3p_z^{0.97}/2s^{0.44}2p_x^{0.01}2p_y^{0.31}2p_z^{0.05}$

From Tables 3 and 4 we observe that the similarities between the $^4\Sigma_u^-$ and the $^2\Sigma_u^-$ states of NLi$_2$ and PLi$_2$ systems are strikingly independent of the level of calculation. At the MRCI level for both molecules the D_e values with respect to ground-state products differ by just 1 kcal/mol while the bond distances by less than 0.005 Å between the $^4\Sigma_u^-$ and $^2\Sigma_u^-$ states.

NLi$_2$, PLi$_2$, ^{2}A$_1$. $(3a_1^24a_1^25a_1^12b_2^2, 5a_1^26a_1^27a_1^13b_2^2)$ These are severely bent states, particularly in the PLi$_2$ system, with LiNLi and LiPLi angles of ~90° and ~67° at all levels of calculation and with D_e values, with respect to the ground-state products of 26.8 and 34.3 kcal/mol, respectively, at the MRCI level of theory (Tables 3 and 4). This is the only state in which the NLi$_2$ species is *unbound* with respect to NLi (X$^3\Sigma^-$) + Li-(^{2}S) fragments, Table 3. The bonding arises from the first excited ^{2}D state of N or P atoms and the ground ^{2}S state of the Li atoms, but the binding scheme is not that clear. The CAS atomic populations are as follows

NLi$_2$: $2s^{1.84}2p_x^{0.0}2p_y^{1.71}2p_z^{1.77}/2s^{0.47}2p_x^{0.0}2p_y^{0.08}2p_z^{0.24}$

PLi$_2$: $3s^{1.87}3p_x^{0.0}3p_y^{1.69}3p_z^{1.63}/2s^{0.47}2p_x^{0.0}2p_y^{0.06}2p_z^{0.28}$

It is interesting that the Li−Li distance within the NLi$_2$ and PLi$_2$ systems is 2.725 and 2.756 Å at the MRCI level, as compared to 2.703 Å of the dilithium molecule Li$_2(^1\Sigma_g^+)$ at the CISD level.

A consistent cartoon with these findings can be drawn as follows

^{2}A$_1$
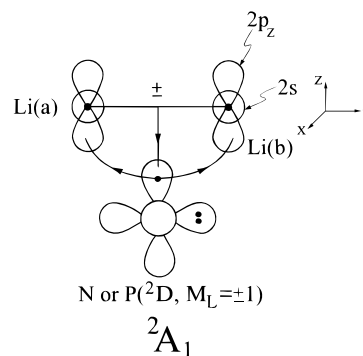
The plus sign of the above cartoon corresponds to a molecular orbital of a$_1$ symmetry and the minus sign to an "antibonding" molecular orbital (MO) of b$_2$ symmetry, while the p$_y$ electron pair on N or P atoms is of b$_2$ symmetry as well. Therefore we can imagine that the bonding is due to a delocalization of the single p$_z$ (N or P) electron into the 2p$_z$(a) + 2p$_z$(b) MO, with a concomitant donation of electrons from the σ-bond (~2s$_a$ + 2s$_b$) of Li$_2$. At the same time the N or P b$_2$ pair can interact with the antibonding system of the Li$_2$ moiety. This picture is in accord with the CAS atomic populations reported previously.

4. Synopsis and Final Remarks

We have examined by ab initio CISD and MRCI techniques, the ground states X̃$^2\Pi_u$ and X̃^{2}B$_1$ and certain low-lying excited states of the NLi$_2$ and PLi$_2$ isovalent species. All states studied, and for both molecules, are bound with respect to the ground-state atoms, N or P(^{4}S) + 2Li(^{2}S). With the exception of the NLi$_2$ ^{2}A$_1$ state, all states for both molecules are also bound with respect to the ground-state fragments NLi or PLi(X$^3\Sigma^-$) + Li-(^{2}S). In addition, all states show ionic character with a total transfer of 0.2−0.5 electrons from the two Li to N or P atoms, depending on the state.

The ground state of NLi$_2$ is linear with a $^2\Pi_u$ symmetry and very floppy, while the PLi$_2$ system, albeit also very floppy, is strongly bent ($\theta = 100°$) with a ground state of ^{2}B$_1$ symmetry and an energy inversion barrier of 2.4 kcal/mol.

At the MRCI level of theory the binding values of NLi$_2$ (X̃$^2\Pi_u$) and PLi$_2$(X̃^{2}B$_1$) are NLi−Li = 51.8 kcal/mol, N−Li (mean) = 42.5 kcal/mol and PLi−Li = 44.1 kcal/mol, P−Li (mean) = 40.2 kcal/mol. The above values should be compared with the D_e values of the ground-state diatomics NLi(X$^3\Sigma^-$) and PLi(X$^3\Sigma^-$) of 33.3 and 36.3 kcal/mol, respectively.

We observe that while the mean binding energies N−Li and P−Li are similar, there is an apparent difference between the NLi−Li and PLi−Li dissociation energies. This is due to the difference in the energy splittings (T_e) A$^3\Pi \leftarrow$ X$^3\Sigma^-$ of NLi and PLi, 5.3 and 13.7 kcal/mol, respectively (MRCI). Comparing the *internal bond strengths*, i.e., dissociation energies for the reactions NLi$_2$(X̃$^2\Pi_u$) → NLi(A$^3\Pi$) + Li(^{2}S) and PLi$_2$($^2\Pi_u$) → PLi(A$^3\Pi$) + Li(^{2}S), the D_e values are 57.1 and 55.4 kcal/mol for the NLi−Li and PLi−Li bonds, respectively. Correcting the 55.4 kcal/mol value by 2.4 kcal/mol due to the energy loss X̃^{2}B$_1$ → $^2\Pi_u$, the PLi−Li internal bond strength becomes 57.8 kcal/mol in practical agreement with the NLi−Li value.

Now, it is of interest to compare the bond length of the ground $^3\Sigma^-$ state of NLi with the corresponding X̃$^2\Pi_u$ of NLi$_2$. At the MRCI level a large bond shortening of 0.103 Å of NLi$_2$ is observed as compared to the bond length of the NLi species, reflecting the difference in the bonding character between the two systems. Using conventional chemical drawings, the two systems can be represented as follows making clear the reason
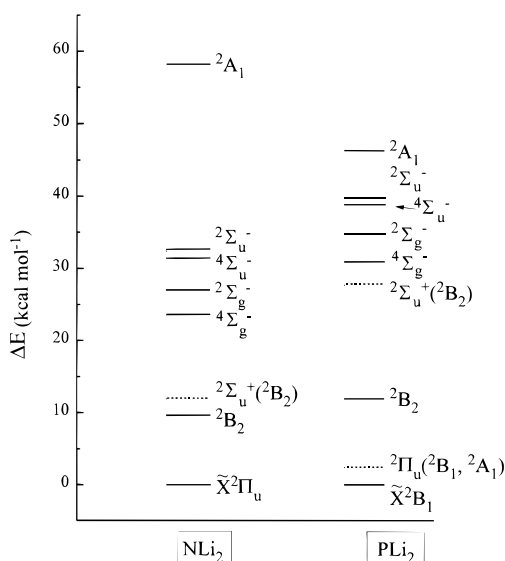
Figure 9. Relative energy diagram for all states computed of the NLi$_2$ and PLi$_2$ species, MRCI level of theory. Dashed levels represent corresponding linear geometries, $^2B_2 \rightarrow {}^2\Sigma_u^+$ (NLi$_2$, PLi$_2$) and $\tilde{X}^2B_1 \rightarrow {}^2\Pi_u$ (PLi$_2$).

$$N\!-\!Li(X^3\Sigma^-) \quad \text{vs.} \quad Li\!-\!N \cdots Li \leftrightarrow Li \cdots N\!-\!Li\,({}^2\Pi_u)$$

of bond shortening in the triatomic molecule. The same is true for the PLi$_2$, PLi systems, but the contrast should be made between the ground $X^3\Sigma^-$ state of PLi and the $^2\Pi_u$ linear configuration of PLi$_2$, not its ground $\tilde{X}^2B_1$ state where the bonding character changes drastically. The bond shortening between PLi($X^3\Sigma^-$) and PLi$_2$($^2\Pi_u$) is 0.107 Å, with the latter being shorter exactly as in the NLi$_2$−NLi case and with the same rationalization.

Finally, Figure 9 shows an energy diagram summarizing relative energy levels for all states and geometries studied for both systems.

References and Notes

(1) Kudo, H.; Zmbov, K. F. *Chem. Phys. Lett.* **1991**, *187*, 77.

(2) Kudo, H. Personal communication. We thank Professor Kudo for providing us with some of his unpublished results on the PLi$_2$ and PLi systems.

(3) See, for instance: Nazri, G. *Solid State Ionics* **1989**, *34*, 97 and references therein.

(4) (a) Tzeli, D.; Papakondylis, A.; Mavridis, A. *J. Mol. Struct.* (*THEOCHEM*) **1997**, *417* (3), 281−291. (b) Matsika, S.; Papakondylis, A.; Mavridis, A. *Chem. Phys. Lett.* **1996**, *250*, 409. (c) Kalemos, A.; Papakondylis, A.; Mavridis, A. *Chem. Phys. Lett.* **1996**, *259*, 185. (d) Kalemos, A.; Papakondylis, A.; Mavridis, A. *J. Mol. Struct.* (*THEOCHEM*) **1995**, *357*, 97. (e) Mavridis, A.; Harrison, J. F. *J. Phys. Chem.* **1982**, *86*, 1979. (f) Mavridis, A.; Harrison, J. F. *J. Am. Chem. Soc.* **1982**, *104*, 3827.

(5) Dunning, T. H., Jr. *J. Chem. Phys.* **1989**, *90*, 1007.

(6) Woon, D. E.; Dunning, T. H., Jr. *J. Chem. Phys.* **1993**, *98*, 1358.

(7) See, for instance: Peterson, K. A.; Dunning, T. H., Jr. *J. Chem. Phys.* **1997**, *106*, 4119. Xantheas, S. S.; Dunning, T. H., Jr.; Mavridis, A. *J. Chem. Phys.* **1997**, *106*, 3280.

(8) Shepard, R.; Shavitt, I.; Pitzer, R. M.; Comeau, D. C.; Pepper, M.; Lischka, H.; Szalay, P. G.; Ahlrichs, R.; Brown, F. B.; Zhao, J.-G. *Int. J. Quantum Chem.* **1988**, *S22*, 149.

(9) Davidson, E. R. *MELD*; Department of Chemistry, Indiana University: Bloomington, IN, 1991.

(10) MOLPRO is a package of ab initio programs written by Werner, H.-J. and Knowles, P. J. with contributions from Almlof, J.; Amos, R. D.; Berning, A.; Deegan, M. J. O.; Eckert, F.; Elbert, S. T.; Hampel, C.; Lindh, R.; Meyer, W.; Nicklass, A.; Peterson, K.; Pitzer, R.; Stone, A. J.; Taylor, P. R.; Mura, M. E.; Pulay, P.; Schuetz, M.; Stoll, H.; Thorsteinsson, T.; and Cooper, D. L.

(11) Werner, H.-J.; Knowles, P. J. *J. Chem. Phys.* **1994**, *89*, 3018. Knowles, P. J.; Werner, H.-J. *Chem. Phys. Lett.* **1988**, *145*, 514. Werner, H.-J.; Reinsch, E. A. *J. Chem. Phys.* **1982**, *76*, 3144. Werner, H.-J. *Adv. Chem. Phys.* **1987**, *69*, 1.

(12) Dykstra, C. E.; Pearson, P. K.; Schaefer, H. F., III. *J. Am. Chem. Soc.* **1975**, *97*, 2321.

(13) (a) Boldyrev, A. I.; Simons, J.; Schleyer, P. v. R. *J. Chem. Phys.* **1993**, *99*, 8793. (b) Boldyrev, A. I.; Simons, J. *J. Phys. Chem.* **1993**, *97*, 6149.

(14) Blomberg, M. R. A.; Siegbahn, P. E. M. *J. Chem. Phys.* **1983**, *78*, 5682.

(15) Moore, C. E. Atomic Energy Levels in: Natl. Stand. Ref. Data Ser., US Natl. Bur. Stand., Cir 35, 1973.